Environmental Science & Technology

Article

Cite This: Environ. Sci. Technol. 2019, 53, 13009−13018

pubs.acs.org/est

Effects of Molecular-Level Compositional Variability in Organic Aerosol on Phase State and Thermodynamic Mixing Behavior

Jenna C. Ditto,[†] Taekyu Joo,[‡] Peeyush Khare,[†] Roger Sheu,[†] Masayuki Takeuchi,[§] Yunle Chen,[‡] Weiqi Xu,[∥,⊥] Alexander A. T. Bui,[#] Yele Sun,[∥] Nga L. Ng,[‡,⊥] and Drew R. Gentner*[,†,¶]

[†]Department of Chemical and Environmental Engineering, Yale University, New Haven, Connecticut 06511, United States

[‡]School of Earth and Atmospheric Sciences, Georgia Institute of Technology, Atlanta, Georgia 30332, United States

[§]School of Civil and Environmental Engineering, Georgia Institute of Technology, Atlanta, Georgia 30332, United States

[∥]State Key Laboratory of Atmospheric Boundary Physics and Atmospheric Chemistry, Institute of Atmospheric Physics, Chinese Academy of Sciences, Beijing 100029, China

[⊥]School of Chemical and Biomolecular Engineering, Georgia Institute of Technology, Atlanta, Georgia 30332, United States

[#]Department of Civil and Environmental Engineering, Rice University, Houston, Texas 77005, United States

[¶]Max Planck Institute for Chemistry, 55128 Mainz, Germany

Supporting Information

ABSTRACT: The molecular-level composition and structure of organic aerosol (OA) affect its chemical/physical properties, transformations, and impacts. Here, we use the molecular-level chemical composition of functionalized OA from three diverse field sites to evaluate the effect of molecular-level compositional variability on OA phase state and thermodynamic mixing favorability. For these ambient sites, modeled aerosol phase state ranges from liquid to semisolid. The observed variability in OA composition has some effect on resulting phase state, but other factors like the presence of inorganic ions, aerosol liquid water, and internal versus external mixing with water are determining factors in whether these particles exist as liquids, semisolids, or solids. Organic molecular composition plays a more important role in determining phase state for phase-separated (verus well-mixed) systems. Similarly, despite the observed OA compositional differences, the thermodynamic mixing favorability for OA samples with aerosol liquid water, isoprene oxidation products, or monoterpene oxidation products remains fairly consistent within each campaign. Mixing of filter-sampled OA and isoprene or monoterpene oxidation products is often favorable in both seasons, while mixing with water is generally unfavorable.

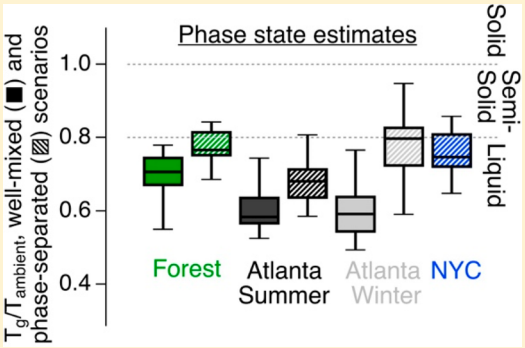

INTRODUCTION

Organic compounds are emitted to the atmosphere in the gas-phase or as primary organic aerosol (POA) from a variety of anthropogenic and biogenic sources. The chemical processing of these organic compounds produces secondary organic aerosol (SOA), a complex and variable mixture of carbon-, hydrogen-, and oxygen-containing species with diverse heteroatom composition and functionality.[1] Organic aerosol (OA) represents a significant fraction of atmospheric particulate matter (20−90%),[2] which is known to be harmful to the respiratory and cardiovascular systems, as well as to contribute to changes in global climate forcing, temperature, and precipitation trends.[3,4] The molecular-level elemental composition and structure of OA directly and indirectly affect its health and environmental impacts by influencing OA chemical/physical properties and transformations in the atmosphere.[3]

While bulk OA composition in the ambient atmosphere (e.g., elemental composition and elemental ratios reported by aerosol mass spectrometers (AMS)) is typically similar over time at a given location, the molecular-level elemental composition of functionalized OA exhibits significant temporal variability.[5] At three diverse field sites in the U.S., 66 ± 13% of functionalized OA compounds differ between consecutive samples; these findings are supported by environmental chamber and modeling studies that show similar variability.[5] This compositional variability is driven by a combination of factors, including differences in emitted gas-phase OA precursors, changes in atmospheric oxidation conditions, and differences in air parcel backward trajectories.[5]

Received: May 7, 2019
Revised: September 13, 2019
Accepted: September 16, 2019
Published: September 16, 2019

DOI: 10.1021/acs.est.9b02664
Environ. Sci. Technol. 2019, 53, 13009−13018

Several OA properties, such as phase state and thermodynamic mixing favorability (via Gibbs free energy of mixing, ΔG_m), are sensitive to elemental and structural composition.[6−19] Molecular size and degree of oxidation influence phase state; larger compounds share more interactions with surrounding compounds, slowing diffusion processes and increasing viscosity, while more oxidized compounds can either increase or decrease viscosity, depending on whether hydrogen bonding or hygroscopicity dominates the behavior, respectively.[6] Similarly, chemical structure influences mixing behavior via differences in dispersion, polarity, and hydrogen bonding intermolecular forces between compounds with different functionality.[9,10,20] Changes in OA phase state may have implications for gas-phase semivolatile organic compound (SVOC) partitioning and equilibrium with the aerosol phase,[10,21,22] including possible associated effects on gas-aerosol or aerosol-water mixing. Combined, these factors may influence the chemical/physical properties and transformations of OA in a given location and associated health and environmental impacts.

Here, we use molecular-level data collected at three diverse field sites to estimate OA phase state and thermodynamic mixing favorability. Specifically, the objectives of this work are to (1) predict and evaluate aerosol phase state using molecular-level elemental composition data from three field sites and two seasons, (2) use molecular-level structural data to estimate the thermodynamic mixing favorability of OA samples in one another and with common trace organic gases, and (3) evaluate the effects of previously observed OA compositional variability (discussed in Ditto et al.[5]) on these two OA properties.

MATERIALS AND METHODS

Sample Collection and Data Acquisition. Daytime and nighttime PM_{10} samples were collected during the summer at three diverse field sites: in a forest in northern Michigan (PROPHET tower, University of Michigan Biological Station), near downtown Atlanta, and in New York City, as previously described.[5] Additional wintertime samples were collected at the Atlanta site (from 1/15/2018−2/18/2018, during the day from 9:00 am to 5:00 pm and at night from 9:00 pm to 5:00 am). All samples were analyzed via liquid chromatography with electrospray ionization (positive and negative mode) and quadrupole time-of-flight mass spectrometry (LC-ESI-Q-TOF). This mass spectrometer (MS) was run in both MS mode (i.e., TOF-only) and MS/MS mode (i.e., tandem MS mode). All site and sampling details, sample preparation steps, instrument operating conditions, data processing, and data quality control procedures are previously described for all summer campaigns and are identical for the Atlanta winter campaign.[5] See Figure S1 for a summary of the methods discussed in this section.

Additional MS/MS spectra were acquired for samples from both summer and winter Atlanta campaigns in both positive and negative ionization mode and used exclusively in thermodynamic mixing favorability analyses. MS spectra were acquired for analytes between m/z 100−1000 at 4 spectra/s, and MS/MS spectra were acquired for analytes between m/z 20−600 at 2 spectra/s. Collision energies were set to 5, 10, 20, 30, and 40 eV. Compounds detected in MS mode (after blank subtraction and peak and formula QC/QA) were specifically targeted by their m/z and retention time in subsequent MS/MS analyses.

Aerosol mass spectrometer (AMS) data were collected for the summertime forest and Atlanta campaigns as previously described[5] but were unavailable for New York City. AMS data were collected in the winter at the Atlanta site, following similar procedures. All AMS data presented here are averaged over corresponding filter sampling periods.

Phase State Modeling. We estimate phase state based on the glass transition temperature parametrization developed by DeRieux and Li et al.[13] This parametrization is based on elemental composition, and accounts for carbon, hydrogen, and oxygen-containing compounds with a relationship determined by multilinear least-squares analysis for measured data from carbon- and hydrogen-containing compounds (CH) and carbon-, hydrogen-, and oxygen-containing compounds (CHO). This relationship is shown in eq 1, where T_g represents glass transition temperature, n_C^0 represents the reference carbon number, and constants n_C, n_H, and n_O represent the number of C, H, and O atoms, respectively. Constants b_C, b_H, and b_O represent the contribution of C, H, and O, respectively, to glass transition temperature. Constants b_{CH} and b_{CO} account for C−H and C−O bond contributions:[13]

$$T_{g,i} = (n_C^0 + \ln(n_C))b_C + \ln(n_H)b_H + \ln(n_C)\ln(n_H)b_{CH} + \ln(n_O)b_O + \ln(n_C)\ln(n_O)b_{CO} \quad (1)$$

Here, we step through the procedure outlined in DeRieux and Li et al., beginning by computing the "dry" mixture-wide glass transition temperature. We start by considering each individual mixture component: in eq 1, we use molecular formulas from LC-ESI-Q-TOF analysis to determine the glass transition temperature of each observed compound. Here, we expand the DeRieux and Li parametrization to include nitrogen- and sulfur-containing compounds, which represent an important proportion of the compounds observed at the 3 sites.[5] Because of the lack of available experimental measurements to robustly parametrize the role of nitrogen/sulfur-containing compounds (which has limited their explicit inclusion in this phase state model), we treat each nitrogen and sulfur atom as a "fraction" of an oxygen atom and perform a Monte Carlo analysis to constrain uncertainty (see Supporting Information).

Dry glass transition temperature ($T_{g,org}$) is calculated according to eq 2, where w_i is the mass fraction of each individual compound, based on DeRieux and Li et al.[13]

$$T_{g,org} = \sum_i w_i T_{g,i} \quad (2)$$

Since the mass fraction of each compound observed is sensitive to ionization efficiency, we perform a sensitivity analysis to evaluate its effects on the overall results (Figure S2).

To account for the influence of water in the atmosphere, we implement the Gordon−Taylor equation (eq 3),[6,13] which incorporates the mass fraction of water ($1 - w_{org}$, eqs 4 and 5), the glass transition temperature of pure water ($T_{g,w}$), the mass fraction of organics (w_{org}, eq 5), the dry glass transition temperature ($T_{g,org}$), and the Gordon−Taylor constant (k_{GT}, an interaction parameter used to describe the glass transition temperature of organic−water mixtures, which can vary based on the mixture's constituents[6,7,23]). We assign each sample a random Gordon−Taylor constant value between 1.05 and 4,[6,7,12,13,23,24] and vary this over each Monte Carlo iteration. Here, $T_g(w_{org})$ represents the overall mixture glass transition temperature:

DOI: 10.1021/acs.est.9b02664
Environ. Sci. Technol. 2019, 53, 13009−13018

$$T_g(w_{org}) = \frac{(1 - w_{org})T_{g,w} + \frac{1}{k_{GT}} w_{org} T_{g,org}}{(1 - w_{org}) + \frac{1}{k_{GT}} w_{org}} \quad (3)$$

OA exists in different possible mixing states with water in the atmosphere depending on chemical composition (organic and inorganic), relative humidity, temperature, and oxidation conditions,[25,26] ranging from phase-separated (i.e., external mixing with water) to well-mixed (i.e., internal mixing with water). While OA may also fall somewhere between these two extremes, we evaluate the extremes to provide an upper and lower limit to OA glass transition temperature, respectively.[27] In the Gordon−Taylor equation, the mass fraction of water comes from organic-derived aerosol liquid water (ALW) for phase-separated particles (eq 4). Following DeRieux and Li et al., we use eqs 4 and 5 with an estimated SOA density (ρ_{SOA}, where ρ_{SOA} = 1.2 g/cm^3), the density of water (ρ_w, where ρ_w = 1 g/cm^3), the mass fraction of SOA (m_{SOA}, computed by converting abundance to concentration using an average response factor and summing individual compound concentrations across each sample[5] or using the AMS organic component concentration, both yield identical results in eqs 4 and 5 when considering organic-derived ALW only), water activity (a_w, where a_w = RH/100), and the effective hygroscpicity parameter (κ). Since the mixture-wide hygroscopicity parameter is unknown, we randomly assign a hygroscopicity parameter value from within an expected range for atmospheric OA (0.01−0.5),[13,28,29] and vary this over each Monte Carlo iteration. Separately, we also consider a more extreme case where the hygroscopicity parameter varies between 0.01 and 0.9.[28,29]

$$m_{H_2O,organic} = \frac{\kappa \rho_w m_{SOA}}{\rho_{SOA}\left(\frac{1}{a_w} - 1\right)} \quad (4)$$

$$w_{org} = \frac{m_{SOA}}{m_{SOA} + m_{H_2O}} \quad (5)$$

For well-mixed particles, water comes from a combination of organic and inorganic sources. We estimate inorganic-derived ALW with ISORROPIA-I, a model that predicts thermodynamic equilibrium between gas- and aerosol-phase species for an ammonium (NH_4^+), sulfate (SO_4^{2-}), nitrate (NO_3^-), chloride (Cl^-), and water (H_2O) system.[27,30,31] ISORROPIA inputs include AMS particle phase data for each of these inorganic ions (where available) and temperature and relative humidity data averaged over the last 6 h of HYSPLIT backward trajectories, as previously described.[5] We assume metastable aerosols and run ISORROPIA in reverse mode.[27] The mass concentration of inorganic ALW, of organic ALW, of each of the AMS inorganic ions, and of organics are all combined in eq 5 to compute the overall mass fraction of organics in this case. For both phase-separated and well-mixed scenarios, the results from eq 5 are used in eq 3 to compute mixture-wide glass transition temperature.

Thermodynamic Mixing Modeling. To evaluate the mixing behavior of each of these OA samples relative to each other and relative to hypothetical isoprene and monoterpene oxidation products, we use MS/MS data to propose chemical structures for each compound, and then compute Hansen Solubility Parameters based on the functional group composition of these structures.[9−11,20] MS/MS spectra were imported to SIRIUS, a structural identification software. CSI:FingerID was used to propose structures for each compound, using isotope patterns from MS data and fragmentation information from MS/MS data.[32,33] We limit possible formula and structural identifications by constraining possible elements (C, H, O, N, S), possible adducts for either positive or negative mode ionization, and mass tolerance to 7 ppm.[5] We compile the top scoring structure for each compound and, then, use the APRL-SSP (APRL Substructure Search Program) developed by Ruggeri and Takahama to enumerate atmospherically relevant functional groups in each compound.[34] With this functional group count, we employ the Hoftyzer−Van Krevelen group contribution method to estimate Hansen Solubility Parameters for dispersion, polarity, and hydrogen bonding intermolecular forces based on functional group-specific molar attraction constants and energies,[20] similar to previous studies that have applied these methods to atmospheric OA.[9−11] This analysis is limited to the functional groups for which tabulated molar attraction constants and energies exist in the literature for the Hoftyzer−Van Krevelen method, with others excluded (tabulated data used here from Van Krevelen and Te Nijenhuis, 2009[20]). This covers an average of 80% of observed species.

Hansen Solubility Parameters are computed for each OA mixture (i.e., sample) according to eqs 6−9:[9,10]

$$\partial_{d,SOA} = \frac{\sum (x_i \sum_k c_k^i F_{d,k})}{\sum x_i V_i} \quad (6)$$

$$\partial_{p,SOA} = \frac{\sqrt{\sum \left(x_i \sum_k c_k^i F_{p,k}{}^2\right)}}{\sum x_i V_i} \quad (7)$$

$$\partial_{hb,SOA} = \sqrt{\frac{\sum (x_i \sum_k c_k^i E_{hb,k})}{\sum x_i V_i}} \quad (8)$$

$$V_i = \sum c_k^i V_k^i \quad (9)$$

In eqs 6−9, ∂_d, ∂_p, ∂_{hb} are the Hansen Solubility Parameters for dispersion, polarity, and hydrogen bonding intermolecular forces, respectively, x is the mole fraction of compound i, c is the number of a particular functional group k, V is molar volume, and F_d, F_p, and E_{hb} are molar attraction constants for each functional group k.

The thermodynamic mixing favorability for each OA mixture can be computed from partial solubility parameters, in addition to information on molar volume, the number of moles of solute and solvent, and temperature:[9,10]

$$\Delta G_m = RT(n_{sl} + mn_o)\chi\phi_{sl}\phi_o - T[-R(n_{sl}\ln(\phi_{sl}) + n_o\ln(\phi_o)] \quad (10)$$

In eq 10, ΔG_m is Gibbs free energy of mixing, R is the universal gas constant, T is temperature, n is number of moles, χ is the Flory−Huggins interaction parameter (which incorporates partial solubility parameters defined in eqs 6−9, see eqs S2−S5), m is a ratio of molar volumes (see Supporting Information), and ϕ is a volume fraction (see Supporting Information). Subscripts sl and o represent solvent and solute, respectively. Equation 10 is used to compute Gibbs free energy of mixing and evaluate the thermodynamic mixing favorability between SOA components: a negative Gibbs free energy of

DOI: 10.1021/acs.est.9b02664
Environ. Sci. Technol. 2019, 53, 13009−13018

mixing indicates favorable mixing, while a positive value indicates unfavorable mixing.

RESULTS AND DISCUSSION

The DeRieux and Li parametrization was developed and validated for CH and CHO compounds.[13] Here, we incorporate nitrogen- and sulfur-containing compounds by treating them similarly to oxygen in the DeRieux and Li parametrization and find that this does not introduce significant uncertainty in resulting dry-phase state estimates (Figure 1). A Monte Carlo analysis yields a small range of dry glass transition temperature (T_g) values and corresponding phase state estimates ($T_g/T_{ambient}$), with a standard deviation that represents 1% the mean, on average. Dry phase state estimates depend only on organic elemental composition (i.e., eqs 1 and 2).

We predict a range of compound-specific glass transition temperatures (Figure S3). The majority of compounds fall between 100 and 400 K, highlighting the diversity of compounds that contribute to overall mixture-wide glass transition temperature. In general, the most frequently occurring compound classes contribute the most to each mixture's dry glass transition temperature (Figure S4). We observe a consistent distribution of glass transition temperatures across campaigns (Figure S3), and relatively consistent dry phase state estimates within each campaign (Figure 1), suggesting that changes in organic elemental composition alone do not dominate particle phase state behavior.

Water in the atmosphere acts as a plasticizer: it has a low glass transition temperature and can reduce the viscosity of OA mixtures.[6] As a result, accounting for water decreases glass transition temperatures and pushes mixture-wide phase state estimates from solid/semisolid "dry" particle behavior toward semisolid and liquid-like behavior. Here, we consider the two extreme cases of well-mixed particles with respect to water (i.e., water contributions from organic- and inorganic-derived ALW) and phase-separated particles (i.e., water contribution from organic-derived ALW only).[27]

Accounting for organic-derived ALW decreases glass transition temperature and increases liquid-like OA behavior, with some temporal phase state fluctuation observed (e.g., Figure 1C). Accounting for both organic- and inorganic-derived ALW (and by extension, the presence of inorganic ions: NO_3^-, SO_4^{2-}, Cl^-, and NH_4^+) decreases the glass transition temperature even further and increases liquid-like behavior, likely because an additional source of water is accounted for in this case. ALW contribution at the Atlanta site during the summer and winter are within the range of previous reported concentrations at the same location.[35]

We observe greater contribution from inorganic ions and inorganic ALW in the Atlanta winter campaign (vs summer), which drives a larger gap between phase-separated and well-mixed phase state estimates. Incorporating inorganic-ALW sometimes stabilizes phase state estimates across samples, particularly in the Atlanta summer and winter campaigns (Figure 1B, samples 23–34; Figure 1C, samples 4–9, 24–30). This is perhaps because while inorganic ALW and inorganic ion concentrations do fluctuate temporally, their $\mu g/m^3$ concentrations far dominate those of the individual organic compounds at ng/m^3 concentrations.

With all contributing factors accounted for, changes in phase state between samples are subtle in most cases, despite larger changes in molecular-level elemental composition. This

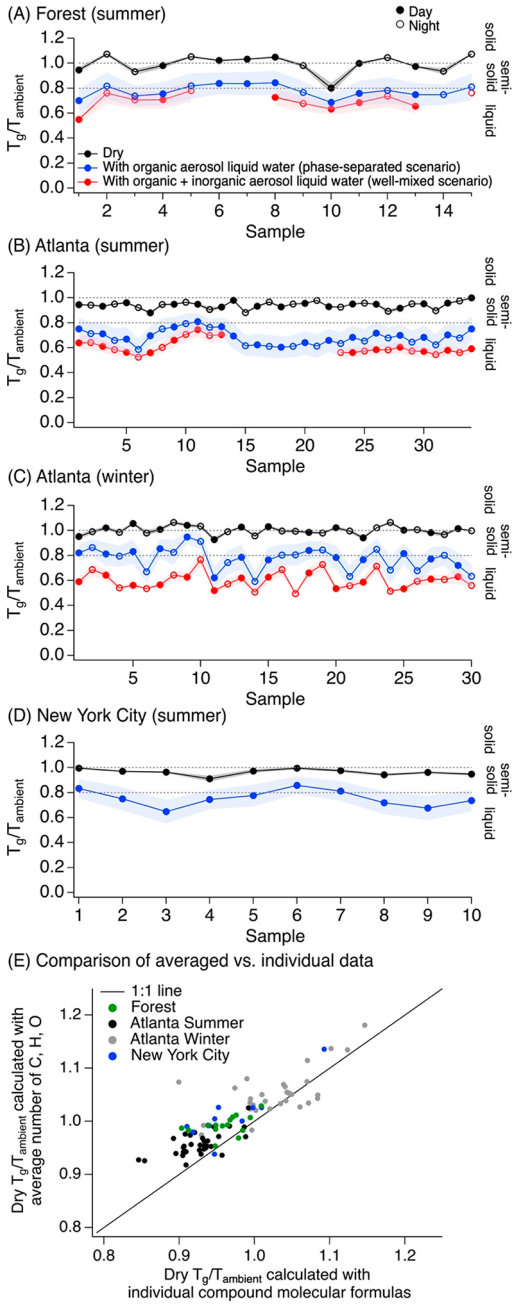

Figure 1. (A–D) Phase state estimates for samples collected at three diverse field sites (samples ordered sequentially) show minimal temporal variation, despite significant changes in molecular-level elemental composition. Glass transition temperatures (T_g) are compared to ambient temperature ($T_{ambient}$), such that solid particles are defined as $T_g/T_{ambient} > 1$, semisolid particles exist in a range between $0.8 < T_g/T_{ambient} < 1$, and liquid particles exist at $T_g/T_{ambient} < 0.8$.[12] A Monte Carlo analysis was performed over 10 000 iterations; markers represent mean results from this analysis (filled in represent daytime samples and open represent nighttime), and shading represents the standard deviation. This standard deviation represents, on average, 8% of $T_g/T_{ambient}$ values for well-mixed estimates, 12% for phase-separated estimates, and 1% for dry estimates. Here, all variables (k_{GT}, κ, treatment of N and S atoms) are varied simultaneously in the Monte Carlo analysis. (E) Dry glass transition temperature estimates computed using individual molecular formulas compared to dry glass transition temperature estimates computed using the average number of carbon, hydrogen, and oxygen atoms across all compounds in a sample (in both cases, for CHO

DOI: 10.1021/acs.est.9b02664
Environ. Sci. Technol. 2019, 53, 13009–13018

Figure 1. continued

compounds only). Using sample-wide average elemental quantities slightly overpredicts dry glass transition temperature compared to using individual molecular formulas, though there is only a 3.5% difference between the two approaches, on average (by campaign, average difference for the forest data is 3.2 ± 2.5%, for Atlanta summer data is 3.2 ± 2.4%, for Atlanta winter is 2.4 ± 4.3%, and for NYC is 4.1 ± 2.8%). These similar results suggest that average elemental composition data may be acceptable for estimating the overall dry glass transition temperature of most, but not all, ambient complex OA mixtures.

indicates that though phase state is sensitive to organic molecular composition, organic molecular composition does not necessarily drive major changes in overall OA phase state. The phase state model used here depends on many other factors, such as relative humidity, the presence/absence of inorganic ions and how they affect the quantity of inorganic ALW present, mixture-wide hygroscopicity, etc. On the basis of these results, it appears that organic composition does not dominate these other factors and thus does not directly control the resulting phase state. Instead, the concentration of NH_4^+ and SO_4^{2-} measured by AMS, as well as total ALW (inorganic and organic) and relative humidity show some correlation with phase state estimates: increasing the contribution of each of these components pushes particle phase state toward liquid-like behavior, while decreasing them pushes particle phase state toward more semisolid/solid behavior (Figure S5). Organic molecular composition plays a more important role in driving phase state for phase-separated particles than for well-mixed ones (Figure S5).

The filter extraction and analysis methods discussed here are tailored for the analysis of functionalized OA. However, nonfunctionalized OA or hydrocarbon-like OA (HOA) may act to stabilize or exacerbate OA compositional variability and associated effects on resulting OA properties, depending on the HOA source. AMS positive matrix factorization (PMF) analysis for the forested site results in 3 factors all associated with oxygenated OA, so no HOA is included for forest estimates.[5] For the Atlanta site, we examine the potential impact of HOA by modeling a hypothetical nonfunctionalized OA fraction using the expected composition of primary organic aerosol (POA) from motor vehicles, with contributions from $C_{16}-C_{34}$ compounds across 7+ double bond equivalents (DBE).[36] Speciated high-resolution mass spectrometry data were not available for $C_{31}-C_{34}$ compounds in previously published work, so we model their contribution based on known relative mass concentrations for each $C_{31}-C_{34}$ carbon number, and the DBE distribution for C_{30} compounds. We then use the HOA concentration from past AMS PMF analysis at the Atlanta site in summer and winter to estimate the relative mass contribution of HOA to the entire OA mixture for each sampling period (using mean concentration ±1 standard deviation).[37,38] This approach does not account for temporal variability in HOA composition. However, nonfunctionalized OA emissions from motor vehicles likely dominate the HOA factor in the Atlanta area, and the composition of motor vehicle emissions is fairly constant regionally with motor oil and diesel fuel.[36,39] Though including HOA in the Atlanta phase state estimates does slightly decrease the resulting mixture-wide glass transition temperature, the effect is very small (Figure S6).

Phase state is sensitive to chemical composition and environmental factors such as temperature and relative humidity and, therefore, varies based on location.[12] The phase states modeled here are similar to previous phase state estimates in similar geographic locations. Previous measurements at the forested site in northern Michigan suggest the presence of semisolid particles at night, transitioning to more liquid-like particles during the day, with overall behavior similar to that observed in the Southeast U.S.[15,27] Although we do not see a distinct diurnal profile in the data presented here, we are considering larger particles than in previous work, which may be less sensitive to diurnal changes.[27] In addition, although the filter samples discussed here are collected during the day and at night, the lifetime of particulate matter in the atmosphere can sometimes reach several days;[3] some of the particles sampled at night may persist from the previous day, and some of the particles sampled during the day may persist from the previous night, making it difficult to discern daytime and nighttime phase state trends with these methods. The forested site contains both coniferous and deciduous trees, resulting in both terpene and isoprene emissions and their oxidation products. Previous studies have observed liquid-like particles in humid isoprene-dominated forests[14] and solid particles in drier monoterpene-dominated forests.[8] In a mixed deciduous/coniferous forest at moderate relative humidity (~60% on average during sampling times), we can expect to see a range of phase state behavior that fits between these two extremes.

Previous summertime measurements in the Southeast U.S. have observed primarily liquid particles, with particles exhibiting semisolid character at lower relative humidity.[15,40] These observations are consistent with the results shown here for the Atlanta site, with summertime phase states estimated as almost exclusively liquid (RH ~72% on average during sampling times), and wintertime phase states varying between liquid and semisolid (RH~62% on average during sampling times).

In the New York City area, we expect phase state behavior characteristic of a mixture of combustion- and non-combustion-related anthropogenic emissions and oxidation products,[41,42] as well as biogenic SOA from regional vegetation.[43] Laboratory studies on anthropogenic precursors show a range of phase behavior depending on the structure of the precursor and degree of oxidation,[18] while recent field measurements in a boreal forest where terpenes are prominent and relative humidity is low suggest solid particles.[8] Thus, with a mixture of SOA sources, degrees of oxidation, and summertime relative humidity in New York City (~61% on average during sampling times), phase states ranging from liquid to semisolid are likely.

Thermodynamic Mixing Favorability. Many factors influence SOA production via the partitioning of gas-phase SVOCs to the particle phase, including thermodynamic limitations to mixing with pre-existing OA.[10,44,45] Using structural data from MS/MS analyses, we apply the Hansen Solubility Framework to Atlanta summer and winter samples to estimate changes in sample-to-sample thermodynamic mixing favorability, along with changes in mixing favorability of ambient OA with water and select isoprene and monoterpene oxidation products. No HOA is included in mixing favorability analyses, as the modeled HOA discussed above does not constrain chemical structure for each carbon- and hydrogen-containing molecular formula.

DOI: 10.1021/acs.est.9b02664
Environ. Sci. Technol. 2019, 53, 13009−13018

When comparing individual samples to each other, treating one as "solute" and one as "solvent" (eqs 6−10), we observe limited variability in thermodynamic mixing favorability (Figure 2) despite significant differences observed in molecular formulas between samples.[5] These sample-to-sample comparisons were selected to investigate variations in sample composition at similar times of day (i.e., similar atmospheric chemical conditions) or between different times of day (i.e., significant changes in atmospheric conditions). Comparison results were similar in most cases, suggesting that although the molecular formulas themselves may be very different from sample-to-sample as previously described, the cumulative effect from the mix of molecular functionalities present remains similar or that the cumulative changes in molecular functionality are not significant enough to affect mixing. In other words, it is possible that the presence of some prominent functional groups (e.g., hydroxyl groups) and structural features (e.g., carbon backbone arrangement) stabilize mixing behavior and/or mixing behavior is less sensitive to the presence/absence of less prominent functional groups (e.g., amines). This is supported by our observation that samples that exhibit unfavorable mixing tend to have large differences

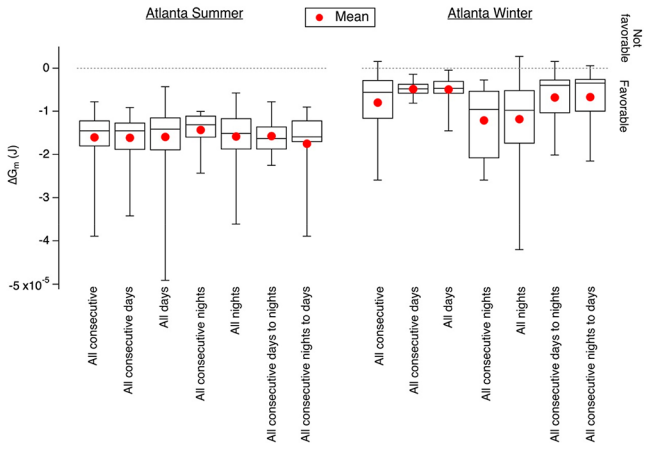

Figure 2. Thermodynamic mixing favorability of each sample compared to other samples within summer or winter Atlanta campaigns (considering organic compounds only), treating one sample as solute and one as solvent. Mixing favorability is expressed as ΔG_m, where a negative ΔG_m indicates favorable mixing and a positive ΔG_m indicates unfavorable mixing. Red markers denote mean ΔG_m for all sample-to-sample comparisons in a given category, and box plot whiskers show maximum and minimum values. There is a distribution of mixing behavior across sample-to-sample comparisons, although most interactions appear to be thermodynamically favorable. Mean ΔG_m values are statistically significantly higher in the winter compared to the same comparison type in the summer (with $p < 0.05$, except in the "all consecutive nights" case where $p > 0.05$); in general, there is more variance in the number of each functional group present in the winter samples, which may contribute to slightly less favorable mixing between samples (Figure S8). In the summer, the contribution from dispersion, polarity, and hydrogen bonding intermolecular forces is similar during the day and at night, resulting in similar mean daytime and nighttime ΔG_m values. In the winter, these intermolecular force contributions are all statistically significantly larger at night compared to during the day, with notable increases in both polarity and hydrogen bonding contributions; polarity and hydrogen bonding intermolecular interactions tend to be strong, and may drive (and increase favorability of) mixing behavior in the winter nighttime samples.

in sample-wide dispersion, polarity, and hydrogen bonding parameters, as well as large differences in molar volume (all directly related to functional group composition).

Additionally, we estimate thermodynamic mixing favorability of filter-sampled OA in inorganic ALW, and the mixing favorability of select hypothetical isoprene and monoterpene oxidation products in filter-sampled OA (compounds at a hypothetical 1 ppt: IEPOX, methyltetrols, methylglyceric acid, pinic acid, pinonic acid, 3-methyl-1,2,3-butanetricarboxylic acid (MBTCA), norpininc acid, pinonaldehyde). While we do not expect to see much contribution from isoprene oxidation products in the winter (i.e., Figure 3E),[37,38] we include the analysis here to examine the sensitivity of wintertime OA to these (and similar) compounds.

OA thermodynamic mixing favorability in water is almost always unfavorable for the Atlanta site (Figure 3A and 3D), which could suggest the presence of phase-separated particles instead of well-mixed ones[17] (though separation between organic rich and inorganic/water rich phases may still be an oversimplification, as the organic rich phase may possess multiple phases as well, for example, limonene SOA together with β-pinene SOA may form a core−shell structure due to SOA viscosity and oligomerization[46]). A previous modeling study in the Southeast U.S. in summer estimates that particles spend roughly 40−70% of the time in a phase-separated state.[26] While we do not directly observe phase separation with these sampling methods, we compare our mixture-wide HSP results (i.e., eqs 6−8) to previous work that uses the HSP framework to characterize phase separation behavior, and observe HSPs in the 20−30 $MPa^{1/2}$ range, which is similar to previous work where phase separation was observed.[11]

If OA mixing with water is indeed thermodynamically unfavorable and if particles do tend toward phase separated behavior, this would result in slightly more variability in phase state with time compared to the well-mixed case (where inorganic ALW and inorganic ions appear to suppress most temporal phase state fluctuation).

The thermodynamic mixing favorability of isoprene and monoterpene oxidation products is generally favorable in all summer and winter samples, with the exception of mixing with methyltetrols exhibiting more variance (likely due to the much larger polarity and hydrogen bonding partial solubility parameters of methyltetrols relative to the rest of the oxidation products considered and relative to the filter-sampled OA).

Particle phase state is known to impact internal diffusion of compounds within particles and the types and rates of heterogeneous reactions that occur.[6,12,47,48] In addition, multiple properties influence a particle's propensity for gas-phase uptake of organic compounds, including particle phase state (driven by viscosity, which can limit gas-phase uptake kinetically),[12,13] mixing favorability (driven by intermolecular forces between compounds, which can limit gas-phase uptake thermodynamically),[10] and volatility (not explicitly discussed here).[44,49] If mixing between two components is theoretically thermodynamically favorable but the particle viscosity is high, it is possible that particle phase state will limit mixing between the two components (i.e., kinetic limitations). Conversely, two components may both be in the liquid phase and, therefore, more amenable mixing, but their chemical structures may make mixing unfavorable (i.e., thermodynamic limitations). We explore the relationship between phase state and mixing favorability for the summer and winter Atlanta campaigns. Here, we focus on phase-separated particles, as Figure 3A, D

DOI: 10.1021/acs.est.9b02664
Environ. Sci. Technol. 2019, 53, 13009−13018

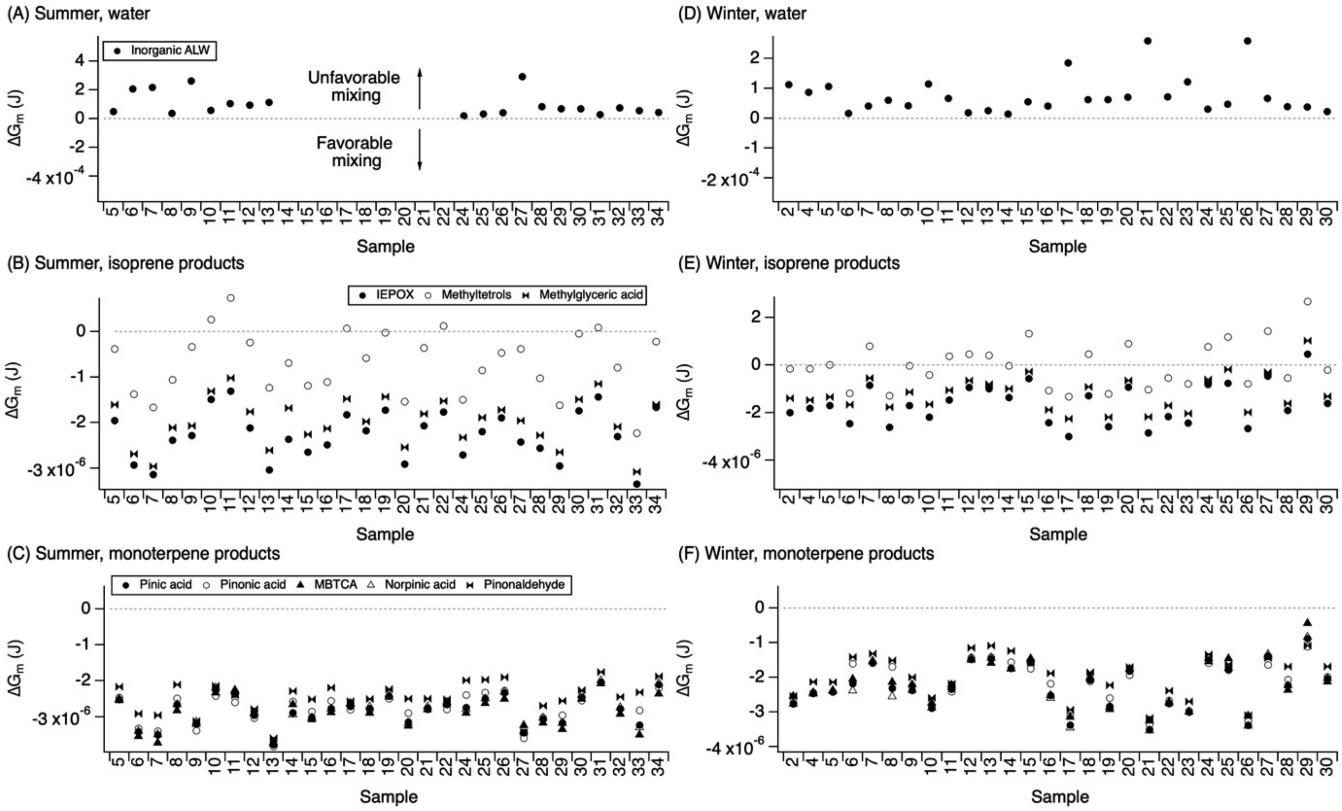

Figure 3. Thermodynamic mixing favorability in Atlanta for each OA sample (organics only) with (A, D) inorganic liquid water, (B, E) with 1 ppt isoprene oxidation products, and (C, F) with 1 ppt monoterpene oxidation products. Negative ΔG_m values suggest favorable mixing. Both summertime and wintertime OA appear to be rarely favorably miscible in water. Isoprene oxidation products tend to mix favorably in the filter-sampled OA in both seasons, with the exception of methyltetrols. Monoterpene oxidation products generally mix favorably in both seasons.

suggests that mixing with water may be thermodynamically unfavorable for the samples discussed here. Phase-separated particles (considering organic ALW only) from the Atlanta campaign range from liquid to semisolid. We observe a few instances where liquid particles may not mix because of their chemical structure/intermolecular forces (i.e., thermodynamic limitations, Figure 4, light gray shading), and also semisolid particles that might mix readily based on thermodynamics alone but that could be limited by particle phase state (i.e., kinetic limitations, Figure 4, dark gray shading). The samples from the Atlanta summer campaigns studied here (when considering the phase-separated scenario) suggest that most interactions between particles in these OA samples are favorable both thermodynamically and kinetically, while mixing between ∼45% of wintertime samples may be kinetically limited due to their semisolid phase state. However, this relationship should be studied at more locations, at different times of day, and during different seasons to better assess the relationship between these two properties in the ambient atmosphere.

Despite large changes in functionalized OA elemental composition across multihour samples at each field site (where 66 ± 13% of compounds are different across sample-to-sample comparisons),[5] we observe relatively less variability in phase state and mixing behavior. This suggests that though these aerosol properties are sensitive to organic chemical composition, day-to-day differences in organic chemical composition alone cause relatively small differences in resulting phase state or thermodynamic mixing behavior. This is particularly true for the well-mixed particle scenario in this study, where particles were predominantly modeled as liquid. The effect of OA compositional variability appears to be larger for phase-separated particles (e.g., Figures 1 and 4), which show more temporal variation in phase state. When comparing phase state estimates computed using individual molecular formulas compared to average elemental distributions (Figure 1E), we observe a 3.5% overprediction using averaged data (with some outlier samples), suggesting that average OA elemental composition data may be acceptable for estimating the phase state of most ambient complex OA mixtures.

Similarly, though there is some variation in Gibbs free energy of mixing values across sample-to-sample comparisons and for mixtures of each sample with water and common isoprene/monoterpene oxidation products, these processes tend to remain fairly consistently favorable or unfavorable within each campaign.

Each individual sample discussed here contains compounds whose exact elemental and structural identities vary significantly from sample to sample, and each of these compounds contributes uniquely to its sample-wide phase state or mixing behavior. However, these results suggest that when all compounds in a sample are pooled together, despite their individual differences within and across samples, the resulting overall mixture behavior (in terms of phase state, whose model is based on elemental composition, and thermodynamic mixing favorability, whose model depends on functional group count) is less affected within each ambient site or season studied here. However, it is possible that estimating phase state and mixing favorability with different models will yield different results; as future methods to characterize these properties are developed,

DOI: 10.1021/acs.est.9b02664
Environ. Sci. Technol. 2019, 53, 13009−13018

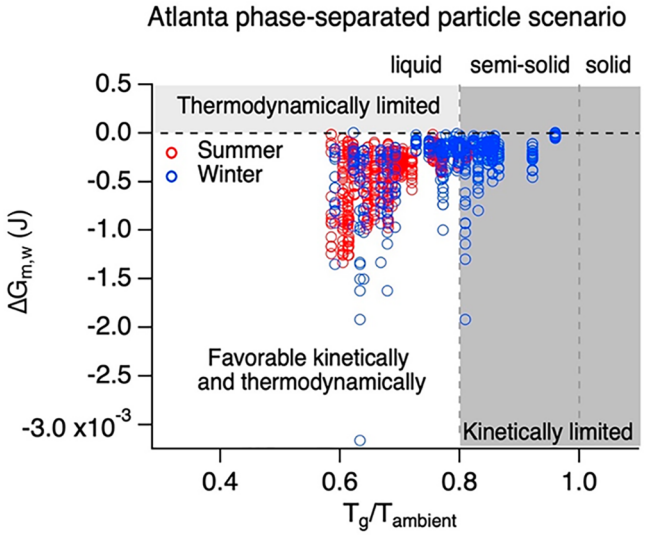

Figure 4. Comparison of thermodynamic mixing favorability (expressed as $\Delta G_{m,w}$, where organic ALW is included along with the organic compounds measured in this OA) and phase state (expressed as $T_g/T_{ambient}$, including organic ALW only) for all sample-to-sample comparisons for Atlanta summer and winter phase separated particles. Sample-to-sample comparisons shown here are the same as shown in Figure 2. Interactions between phase-separated particles appear rarely limited by thermodynamics, but kinetic limitations are likely for semisolid particles that are prevalent in the winter campaign. The phase state of the sample treated as the "solvent" in each sample-to-sample computation of $\Delta G_{m,w}$ is shown here (i.e., from eq 10); see Figure S9 for similar results when considering the "solute's" phase state. Light gray shading highlights a region where mixing is thermodynamically unfavorable. Dark gray shading highlights a region where mixing is likely limited by kinetics due to semisolid/solid particles and their correspondingly high viscosity.

results should be compared and contrasted across approaches to gain a fuller understanding of OA behavior in the atmosphere.

Future studies that investigate more ambient locations across seasons and diurnally are necessary to further investigate the relationship between OA compositional variability and other resulting aerosol properties. In addition, future work that robustly parametrizes nitrogen and sulfur to estimate phase state and establishes thermodynamic mixing behavior for a wider range of functional groups would increase the breadth of OA compounds that can be directly modeled and characterized in terms of these two properties.

However, on the basis of the results from these three sites, future models that incorporate phase state and mixing estimates can approximate phase and mixing behavior with current parametrizations that depend only on elemental and functional group count, despite any underlying variation in molecular-level mixture composition that is not reflected in these metrics.

■ ASSOCIATED CONTENT

Supporting Information

The Supporting Information is available free of charge on the ACS Publications website at DOI: 10.1021/acs.est.9b02664.

Supplemental methods details, distribution of dry glass transition temperatures, contribution of different compound classes to dry glass transition temperature, driving factors of phase state variation, influence of HOA on phase state estimates, viscosity estimates, functional group variation between samples, and additional analysis of the relationship between phase state and mixing favorability (PDF)

■ AUTHOR INFORMATION

Corresponding Author

*E-mail: drew.gentner@yale.edu.

ORCID

Jenna C. Ditto: 0000-0001-6531-4412
Taekyu Joo: 0000-0002-8252-4232
Peeyush Khare: 0000-0003-1078-1296
Yunle Chen: 0000-0001-9904-2638
Yele Sun: 0000-0003-2354-0221
Nga L. Ng: 0000-0001-8460-4765
Drew R. Gentner: 0000-0003-3066-2614

Author Contributions

J.C.D. and D.R.G. designed the study and led analysis. J.C.D. collected filter samples at the forested site. A.A.T.B. collected and analyzed AMS data at the forested site. T.J. collected filter samples at the Atlanta site, and T.J., Y.C., M.T., W.X., and N.L.N. collected and analyzed AMS data for the Atlanta site. P.K. collected filter samples in New York City. R.S. contributed to functional group enumeration methods. Y.S. contributed to refining phase state and thermodynamic mixing discussion. J.C.D. analyzed all filter data and compiled all modeling results. J.C.D. and D.R.G. wrote the paper, and all authors contributed to refining the manuscript.

Notes

The authors declare no competing financial interest.

■ ACKNOWLEDGMENTS

We would like to thank Daniel Knopf, Manabu Shiraiwa, Jonathan Slade, Arthur Chan, and Jianhuai Ye for helpful discussions, and Robert Griffin for providing helpful comments and AMS data from the PROPHET site. We also thank the University of Michigan Biological Station and the New York State Department of Environmental Conservation for enabling us to collect samples at these two locations. We gratefully acknowledge the NOAA Air Resources Laboratory (ARL) for the provision of the HYSPLIT transport and dispersion model and READY website (http://www.ready.noaa.gov) used in this publication for temperature and relative humidity data. D.R.G. and J.C.D. acknowledge support from National Science Foundation Award 1622389, National Science Foundation Award AWD0001666, and the Alexander von Humboldt Foundation. T.J., M.T, Y.C., and N.L.N. acknowledge support from National Science Foundation CAREER AGS-1555034.

■ REFERENCES

(1) O'Brien, R. E.; Laskin, A.; Laskin, J.; Liu, S.; Weber, R.; Russell, L. M.; Goldstein, A. H. Molecular characterization of organic aerosol using nanospray desorption/electrospray ionization mass spectrometry: CalNex 2010 field study. *Atmos. Environ.* **2013**, *68*, 265−272.

(2) Jimenez, J. L.; Canagaratna, M. R.; Donahue, N. M.; Prevot, A. S. H.; Zhang, Q.; Kroll, J. H.; Decarlo, P. F.; Allan, J. D.; Coe, H.; Ng, N. L.; Aiken, A. C.; Docherty, K. S.; Ulbrich, I. M.; Grieshop, A. P.; Robinson, A. L.; Duplissy, J.; Smith, J. D.; Wilson, K. R.; Lanz, V. A.; et al. Evolution of Organic Aerosols in the Atmosphere. *Science* **2009**, *326*, 1525−1529.

DOI: 10.1021/acs.est.9b02664
Environ. Sci. Technol. 2019, 53, 13009−13018

(3) Hallquist, M.; Wenger, J. C.; Baltensperger, U.; Rudich, Y.; Simpson, D.; Claeys, M.; Dommen, J.; Donahue, N. M.; George, C.; Goldstein, A. H.; Hamilton, J. F.; Herrmann, H.; Hoffmann, T.; Iinuma, Y.; Jang, M.; Jenkin, M. E.; Jimenez, J. L.; Kiendler-Scharr, A.; Maenhaut, W.; et al. The formation, properties and impact of secondary organic aerosol: current and emerging issues. *Atmos. Chem. Phys.* **2009**, *9*, 5155−5236.
(4) Pöschl, U.; Shiraiwa, M. Multiphase Chemistry at the Atmosphere-Biosphere Interface Influencing Climate and Public Health in the Anthropocene. *Chem. Rev.* **2015**, *115*, 4440−4475.
(5) Ditto, J. C.; Barnes, E. B.; Khare, P.; Takeuchi, M.; Joo, T.; Bui, A. A. T.; Lee-Taylor, J.; Eris, G.; Chen, Y.; Aumont, B.; Jimenez, J. L.; Ng, N. L.; Griffin, R. J.; Gentner, D. R. An omnipresent diversity and variability in the chemical composition of atmospheric functionalized organic aerosol. *Commun. Chem.* **2018**, *1*, 75.
(6) Koop, T.; Bookhold, J.; Shiraiwa, M.; Pöschl, U. Glass transition and phase state of organic compounds: dependency on molecular properties and implications for secondary organic aerosols in the atmosphere. *Phys. Chem. Chem. Phys.* **2011**, *13*, 19238−19255.
(7) Zobrist, B.; Marcolli, C.; Pedernera, D. A.; Koop, T. Do atmospheric aerosols form glasses? *Atmos. Chem. Phys.* **2008**, *8*, 5221−5244.
(8) Virtanen, A.; Joutsensaari, J.; Koop, T.; Kannosto, J.; Yli-Pirilä, P.; Leskinen, J.; Mäkelä, J. M.; Holopainen, J. K.; Pöschl, U.; Kulmala, M.; Worsnop, D. R.; Laaksonen, A. An amorphous solid state of biogenic secondary organic aerosol particles. *Nature* **2010**, *467*, 824−827.
(9) Jang, M.; Kamens, R. M.; Leach, K. B.; Strommen, M. R. A thermodynamic approach using group contribution methods to model the partitioning of semivolatile organic compounds on atmospheric particulate matter. *Environ. Sci. Technol.* **1997**, *31*, 2805−2811.
(10) Ye, J.; Gordon, C. A.; Chan, A. W. H. Enhancement in Secondary Organic Aerosol Formation in the Presence of Preexisting Organic Particle. *Environ. Sci. Technol.* **2016**, *50*, 3572−3579.
(11) Ye, J.; Van Rooy, P.; Adam, C. H.; Jeong, C.-H.; Urch, B.; Cocker, D. R.; Evans, G. J.; Chan, A. W. H. Predicting Secondary Organic Aerosol Enhancement in the Presence of Atmospherically Relevant Organic Particles. *ACS Earth Sp. Chem.* **2018**, *2*, 1035−1046.
(12) Shiraiwa, M.; Li, Y.; Tsimpidi, A. P.; Karydis, V. A.; Berkemeier, T.; Pandis, S. N.; Lelieveld, J.; Koop, T.; Pöschl, U. Global distribution of particle phase state in atmospheric secondary organic aerosols. *Nat. Commun.* **2017**, *8*, 15002.
(13) DeRieux, W.-S. W.; Li, Y.; Lin, P.; Laskin, J.; Laskin, A.; Bertram, A. K.; Nizkorodov, S. A.; Shiraiwa, M. Predicting the glass transition temperature and viscosity of secondary organic material using molecular composition. *Atmos. Chem. Phys.* **2018**, *18*, 6331−6351.
(14) Bateman, A. P.; Gong, Z.; Liu, P.; Sato, B.; Cirino, G.; Zhang, Y.; Artaxo, P.; Bertram, A. K.; Manzi, A. O.; Rizzo, L. V.; Souza, R. A. F.; Zaveri, R. A.; Martin, S. T. Sub-micrometre particulate matter is primarily in liquid form over Amazon rainforest. *Nat. Geosci.* **2016**, *9*, 34−37.
(15) Pajunoja, A.; Hu, W.; Leong, Y. J.; Taylor, N. F.; Miettinen, P.; Palm, B. B.; Mikkonen, S.; Collins, D. R.; Jimenez, J. L.; Virtanen, A. Phase state of ambient aerosol linked with water uptake and chemical aging in the southeastern US. *Atmos. Chem. Phys.* **2016**, *16*, 11163−11176.
(16) Kidd, C.; Perraud, V.; Wingen, L. M.; Finlayson-Pitts, B. J. Integrating phase and composition of secondary organic aerosol from the ozonolysis of a-pinene. *Proc. Natl. Acad. Sci. U. S. A.* **2014**, *111*, 7552−7557.
(17) Freedman, M. A. Phase separation in organic aerosol. *Chem. Soc. Rev.* **2017**, *46*, 7694−7705.
(18) Saukko, E.; Lambe, A. T.; Massoli, P.; Koop, T.; Wright, J. P.; Croasdale, D. R.; Pedernera, D. A.; Onasch, T. B.; Laaksonen, A.; Davidovits, P.; Worsnop, D. R.; Virtanen, A. Humidity-dependent phase state of SOA particles from biogenic and anthropogenic precursors. *Atmos. Chem. Phys.* **2012**, *12*, 7517−7529.
(19) Renbaum-Wolff, L.; Grayson, J. W.; Bateman, A. P.; Kuwata, M.; Sellier, M.; Murray, B. J.; Shilling, J. E.; Martin, S. T.; Bertram, A. K. Viscosity of a-pinene secondary organic material and implications for particle growth and reactivity. *Proc. Natl. Acad. Sci. U. S. A.* **2013**, *110*, 8014−8019.
(20) Van Krevelen, D. W.; Te Nijenhuis, K. *Properties of Polymers*; Elsevier, 2009.
(21) Mai, H.; Shiraiwa, M.; Flagan, R. C.; Seinfeld, J. H. Under What Conditions Can Equilibrium Gas-Particle Partitioning Be Expected to Hold in the Atmosphere? *Environ. Sci. Technol.* **2015**, *49*, 11485−11491.
(22) Liu, P.; Li, Y. J.; Wang, Y.; Bateman, A. P.; Zhang, Y.; Gong, Z.; Bertram, A. K.; Martin, S. T. Highly Viscous States Affect the Browning of Atmospheric Organic Particulate Matter. *ACS Cent. Sci.* **2018**, *4*, 207−215.
(23) Lessmeier, J.; Dette, H. P.; Godt, A.; Koop, T. Physical state of 2-methylbutane-1,2,3,4-tetraol in pure and internally mixed aerosols. *Atmos. Chem. Phys.* **2018**, *18*, 15841−15857.
(24) Dette, H. P.; Koop, T. Glass formation processes in mixed inorganic/organic aerosol particles. *J. Phys. Chem. A* **2015**, *119*, 4552−4561.
(25) Song, M.; Marcolli, C.; Krieger, U. K.; Zuend, A.; Peter, T. Liquid-liquid phase separation in aerosol particles: Dependence on O:C, organic functionalities, and compositional complexity. *Geophys. Res. Lett.* **2012**, *39*, L19801.
(26) Pye, H. O. T.; Murphy, B. N.; Xu, L.; Ng, N. L.; Carlton, A. G.; Guo, H.; Weber, R.; Vasilakos, P.; Appel, K. W.; Budisulistiorini, S. H.; Surratt, J. D.; Nenes, A.; Hu, W.; Jimenez, J. L.; Isaacman-VanWertz, G.; Misztal, P. K.; Goldstein, A. H. On the implications of aerosol liquid water and phase separation for organic aerosol mass. *Atmos. Chem. Phys.* **2017**, *17*, 343−369.
(27) Slade, J. H.; Ault, A. P.; Bui, A. T.; Ditto, J. C.; Lei, Z.; Bondy, A. L.; Olson, N. E.; Cook, R. D.; Desrochers, S. J.; Harvey, R. M.; Erickson, M. H.; Wallace, H. W.; Alvarez, S. L.; Flynn, J. H.; Boor, B. E.; Petrucci, G. A.; Gentner, D. R.; Griffin, R. J.; Shepson, P. B. Bouncier Particles at Night: Biogenic Secondary Organic Aerosol Chemistry and Sulfate Drive Diel Variations in the Aerosol Phase in a Mixed Forest. *Environ. Sci. Technol.* **2019**, *53*, 4977−4987.
(28) Petters, M. D.; Kreidenweis, S. M. A single parameter representation of hygroscopic growth and cloud condensation nucleus activity. *Atmos. Chem. Phys.* **2007**, *7*, 1961−1971.
(29) Petters, M. D.; Kreidenweis, S. M. A single parameter representation of hygroscopic growth and cloud condensation nucleus activity - Part 2: Including solubility. *Atmos. Chem. Phys.* **2008**, *8*, 6273−6279.
(30) Nenes, A.; Pandis, S. N.; Pilinis, C. ISORROPIA: A New Thermodynamic Equilibrium Model for Multiphase Multicomponent Inorganic Aerosols. *Aquat. Geochem.* **1998**, *4*, 123−152.
(31) Fountoukis, C.; Nenes, A. ISORROPIA II: a computationally efficient thermodynamic equilibrium model for K+−Ca2+−Mg2+−NH4+−Na+−SO42−−NO3−−Cl−−H2O aerosols. *Atmos. Chem. Phys.* **2007**, *7*, 4639−4659.
(32) Dührkop, K.; Shen, H.; Meusel, M.; Rousu, J.; Böcker, S. Searching molecular structure databases with tandem mass spectra using CSI:FingerID. *Proc. Natl. Acad. Sci. U. S. A.* **2015**, *112*, 12580−12585.
(33) Shen, H.; Dührkop, K.; Böcker, S.; Rousu, J. Metabolite identification through multiple kernel learning on fragmentation trees. *Bioinformatics* **2014**, *30*, 157−164.
(34) Ruggeri, G.; Takahama, S. Technical Note: Development of chemoinformatic tools to enumerate functional groups in molecules for organic aerosol characterization. *Atmos. Chem. Phys.* **2016**, *16*, 4401−4422.
(35) Guo, H.; Xu, L.; Bougiatioti, A.; Cerully, K. M.; Capps, S. L.; Hite, J. R.; Carlton, A. G.; Lee, S. H.; Bergin, M. H.; Ng, N. L.; Nenes, A.; Weber, R. J. Fine-particle water and pH in the southeastern United States. *Atmos. Chem. Phys.* **2015**, *15*, 5211−5228.
(36) Worton, D. R.; Isaacman, G.; Gentner, D. R.; Dallmann, T. R.; Chan, A. W. H.; Ruehl, C.; Kirchstetter, T. W.; Wilson, K. R.; Harley,

DOI: 10.1021/acs.est.9b02664
Environ. Sci. Technol. 2019, 53, 13009−13018

R. A.; Goldstein, A. H. Lubricating Oil Dominates Primary Organic Aerosol Emissions from Motor Vehicles. *Environ. Sci. Technol.* **2014**, *48*, 3698−3706.
(37) Xu, L.; Guo, H.; Boyd, C. M.; Klein, M.; Bougiatioti, A.; Cerully, K. M.; Hite, J. R.; Isaacman-VanWertz, G.; Kreisberg, N. M.; Knote, C.; Olson, K.; Koss, A.; Goldstein, A. H.; Hering, S. V.; De Gouw, J.; Baumann, K.; Lee, S.-H.; Nenes, A.; Weber, R. J.; et al. Effects of anthropogenic emissions on aerosol formation from isoprene and monoterpenes in the southeastern United States. *Proc. Natl. Acad. Sci. U. S. A.* **2015**, *112*, 37−42.
(38) Xu, L.; Suresh, S.; Guo, H.; Weber, R. J.; Ng, N. L. Aerosol characterization over the southeastern United States using high-resolution aerosol mass spectrometry: spatial and seasonal variation of aerosol composition and sources with a focus on organic nitrates. *Atmos. Chem. Phys.* **2015**, *15*, 7307−7336.
(39) Gentner, D. R.; Isaacman, G.; Worton, D. R.; Chan, A. W. H.; Dallmann, T. R.; Davis, L.; Liu, S.; Day, D. A.; Russell, L. M.; Wilson, K. R.; Weber, R.; Guha, A.; Harley, R. A.; Goldstein, A. H. Elucidating secondary organic aerosol from diesel and gasoline vehicles through detailed characterization of organic carbon emissions. *Proc. Natl. Acad. Sci. U. S. A.* **2012**, *109*, 18318−18323.
(40) Reid, J. P.; Bertram, A. K.; Topping, D. O.; Laskin, A.; Martin, S. T.; Petters, M. D.; Pope, F. D.; Rovelli, G. The viscosity of atmospherically relevant organic particles. *Nat. Commun.* **2018**, *9*, 956.
(41) Khare, P.; Gentner, D. R. Considering the future of anthropogenic gas-phase organic compound emissions and the increasing influence of non-combustion sources on urban air quality. *Atmos. Chem. Phys.* **2018**, *18*, 5391−5413.
(42) McDonald, B. C.; de Gouw, J. A.; Gilman, J. B.; Jathar, S. H.; Akherati, A.; Cappa, C. D.; Jimenez, J. L.; Lee-Taylor, J.; Hayes, P. L.; McKeen, S. A.; Cui, Y. Y.; Kim, S.-W.; Gentner, D. R.; Isaacman-VanWertz, G.; Goldstein, A. H.; Harley, R. A.; Roberts, J. M.; Frost, G. J.; Ryerson, T. B.; et al. Volatile chemical products emerging as largest petrochemical source of urban organic emissions. *Science* **2018**, *359*, 760−764.
(43) Sun, Y. L.; Zhang, Q.; Schwab, J. J.; Demerjian, K. L.; Chen, W. N.; Bae, M. S.; Hung, H. M.; Hogrefe, O.; Frank, B.; Rattigan, O. V.; Lin, Y. C. Characterization of the sources and processes of organic and inorganic aerosols in New York city with a high-resolution time-of-flight aerosol mass spectrometer. *Atmos. Chem. Phys.* **2011**, *11*, 1581−1602.
(44) Ye, Q.; Upshur, M. A.; Robinson, E. S.; Geiger, F. M.; Sullivan, R. C.; Thomson, R. J.; Donahue, N. M. Following Particle-Particle Mixing in Atmospheric Secondary Organic Aerosols by Using Isotopically Labeled Terpenes. *Chem.* **2018**, *4*, 318−333.
(45) Gong, Z.; Han, Y.; Liu, P.; Ye, J.; Keutsch, F. N.; McKinney, K. A.; Martin, S. T. Influence of Particle Physical State on the Uptake of Medium-Sized Organic Molecules. *Environ. Sci. Technol.* **2018**, *52*, 8381−8389.
(46) Boyd, C. M.; Nah, T.; Xu, L.; Berkemeier, T.; Ng, N. L. Secondary Organic Aerosol (SOA) from Nitrate Radical Oxidation of Monoterpenes: Effects of Temperature, Dilution, and Humidity on Aerosol Formation, Mixing, and Evaporation. *Environ. Sci. Technol.* **2017**, *51*, 7831−7841.
(47) Kuwata, M.; Martin, S. T. Phase of atmospheric secondary organic material affects its reactivity. *Proc. Natl. Acad. Sci. U. S. A.* **2012**, *109*, 17354−17359.
(48) Li, Y. J.; Liu, P.; Gong, Z.; Wang, Y.; Bateman, A. P.; Bergoend, C.; Bertram, A. K.; Martin, S. T. Chemical Reactivity and Liquid/Nonliquid States of Secondary Organic Material. *Environ. Sci. Technol.* **2015**, *49*, 13264−13274.
(49) Liu, P.; Li, Y. J.; Wang, Y.; Gilles, M. K.; Zaveri, R. A.; Bertram, A. K.; Martin, S. T. Lability of secondary organic particulate matter. *Proc. Natl. Acad. Sci. U. S. A.* **2016**, *113*, 12643−12648.

DOI: 10.1021/acs.est.9b02664
Environ. Sci. Technol. 2019, 53, 13009−13018